4658 *Inorg. Chem.* **2009,** *48,* 4658–4660
DOI:10.1021/ic900517u

Inorganic Chemistry
Communication

Use of Hydrazine in the Hydrothermal Synthesis of Chalcogenides: the Neutral Framework Material $[Mn_2SnS_4(N_2H_4)_2]$

Manolis J. Manos and Mercouri G. Kanatzidis*

Department of Chemistry, Northwestern University, 2145 Sheridan Road, Evanston, Illinois 6020-3113

Received March 16, 2009

The reaction system Mn/Sn/S/hydrazine/water at ~150 °C afforded $[Mn_2SnS_4(N_2H_4)_2]$ (**1**). The compound has a unique neutral three-dimensional framework with bridging hydrazine ligands and a variety of interconnectivity modes between MnL_6 (L = N, S) octahedra. The complex structure of **1** leads to strong antiferromagnetic interactions between the Mn^{2+} centers and ordering at ~41 K. The stabilization of **1** underscores the high potential of hydrazine to promote the formation of novel chalcogenide materials under solvothermal conditions.

Intense research efforts are now devoted to the synthesis of new polymeric metal chalcogenide compounds.[1] The interest in these materials stems not only from their unique structure types and topologies,[2] but also from their potential applications in fields as diverse as electronics,[3] nonlinear optics,[4] photoluminescence,[5] catalysis,[6] ionic conduction,[7] magnetism,[8] thermoelectrics,[9] porous materials,[10] and ion exchange.[11] Synthesis under relatively mild conditions, such as solvothermal[2d] or flux[2a] methods, provides a proven way to achieve the isolation of new materials with unusual structures and interesting physical properties.[12]

A number of homo- and heterobimetallic chalcogenides with layered and three-dimensional framework structures have been prepared by reacting metals or binary metal chalcogenides and chalcogens in the presence of an organic amine under hydrothermal conditions.[10,13] The vast majority of these are anionic including protonated amines as the counterions located in the pores or interlayer space of the framework. The solvothermal approach allows the innovative choice of solvents to stabilize unusual structures. Here we report on the use of hydrazine and its role in yielding a neutral framework.

We have isolated the neutral chalcogenide framework material $[Mn_2SnS_4(N_2H_4)_2]$ (**1**) from the reaction performed in a hydrazine/water solvent at 150 °C. The compound is unique because it contains hydrazine as an integral part of the framework as opposed to being located in the pores.[14] **1** exhibits a new three-dimensional structure with bridging hydrazine ligands and various interconnectivity modes between the metal ions. Although the number of chalcogenide compounds with hydrazine ligands prepared

*To whom correspondence should be addressed. E-mail: m-kanatzidis@northwestern.edu.

(1) (a) Kim, Y.; Seo, I. S.; Martin, S. W.; Baek, J.; Halasyamani, P. S.; Arumugam, N.; Steinfink, H. *Chem. Mater.* **2008**, *20*, 6048–6052. (b) Li, H. L.; Kim, J.; O'Keeffe, M.; Yaghi, O. M. *Angew. Chem., Int. Ed.* **2003**, *42*, 1819–1821. (c) Mohanan, J. L.; Arachchige, I. U.; Brock, S. L. *Science* **2005**, *307*, 397–400. (d) Kim, J. Y.; Hughbanks, T. *Inorg. Chem.* **2000**, *39*, 3092–3097. (e) Gray, D. L.; Long, G. J.; Grandjean, F.; Hermann, R. P.; Ibers, J. A. *Inorg. Chem.* **2008**, *47*, 94–100. (f) Scott, R. W. J.; MacLachlan, M. J.; Ozin, G. A. *Curr. Opin. Solid State Mater. Sci.* **1999**, *4*, 113–121. (g) Choudhury, A.; Dorhout, P. K. *Inorg. Chem.* **2008**, *47*, 3603–3609.

(2) (a) Kanatzidis, M. G.; Sutorik, A. C. *Prog. Inorg. Chem.* **1995**, *43*, 151–265. (b) Bu, X. H.; Zheng, N. F.; Feng, P. Y. *Chem.—Eur. J.* **2004**, *10*, 3356–3362. (c) Dehnen, S.; Melullis, M. *Coord. Chem. Rev.* **2007**, *251*, 1259–1280. (d) Sheldrick, W. S.; Wachhold, M. *Angew. Chem., Int. Ed.* **1997**, *36*, 207–224. (e) Stephan, H. O.; Kanatzidis, M. G. *J. Am. Chem. Soc.* **1996**, *118*, 12226.

(3) Mitzi, D. B.; Kosbar, L. L.; Murray, C. E.; Copel, M.; Afzali, A. *Nature (London)* **2004**, *428*, 299–303.

(4) Bera, T. K.; Song, J. H.; Freeman, A. J.; Jang, J. I.; Ketterson, J. B.; Kanatzidis, M. G. *Angew. Chem., Int. Ed.* **2008**, *47*, 7828–7832.

(5) Wu, M.; Emge, T. J.; Huang, X. Y.; Li, J.; Zhang, Y. *J. Solid State Chem.* **2008**, *181*, 415–422.

(6) (a) Zheng, N.; Bu, X. H.; Vu, H.; Feng, P. Y. *Angew. Chem., Int. Ed.* **2005**, *44*, 5299–5303. (b) Kanatzidis, M. G.; Huang, S. P. *Inorg. Chem.* **1989**, *28*, 4667–4669.

(7) Zheng, N. F.; Bu, X. H.; Feng, P. Y. *Nature (London)* **2003**, *426*, 428–432.

(8) Aitken, J. A.; Cowen, J. A.; Kanatzidis, M. G. *Chem. Mater.* **1998**, *10*, 3928–3935.

(9) Hsu, K. F.; Loo, S.; Guo, F.; Chen, W.; Dyck, J. S.; Uher, C.; Hogan, T.; Polychroniadis, E. K.; Kanatzidis, M. G. *Science* **2004**, *303*, 818–821.

(10) (a) Zheng, N. F.; Bu, X. G.; Wang, B.; Feng, P. Y. *Science* **2002**, *298*, 2366–2369. (b) Bag, S.; Trikalitis, P. N.; Chupas, P. J.; Armatas, G. S.; Kanatzidis, M. G. *Science* **2007**, *317*, 490–493.

(11) (a) Manos, M. J.; Chrissafis, K.; Kanatzidis, M. G. *J. Am. Chem. Soc.* **2006**, *128*, 8875–8883. (b) Manos, M. J.; Ding, N.; Kanatzidis, M. G. *Proc. Natl. Acad. Sci. U.S.A.* **2008**, *105*, 3696–3699. (c) Manos, M. J.; Petkov, V.; Kanatzidis, M. G. *Adv. Funct. Mater.* **2009**, *19*, 1087–1092. (d) Manos, M. J.; Iyer, R. G.; Quarez, E.; Liao, J. H.; Kanatzidis, M. G. *Angew. Chem., Int. Ed.* **2005**, *44*, 3552–3555.

(12) Kanatzidis, M. G.; Poeppelmeier, K. R. *Prog. Solid State Chem.* **2008**, *36*, 1–133.

(13) (a) Cahill, C. L.; Parise, J. B. *Dalton Trans.* **2000**, 1475–1482. (b) Manos, M. J.; Malliakas, C. D.; Kanatzidis, M. G. *Chem.—Eur. J.* **2007**, *13*, 51–58. (c) Zheng, N. F.; Bu, X. H.; Feng, P. Y. *Chem. Commun.* **2005**, 2805–2807. (d) Manos, M. J.; Jang, J. I.; Ketterson, J. B.; Kanatzidis, M. G. *Chem. Commun.* **2008**, 972–974. (e) Bowes, C. L.; Petrov, S.; Vovk, G.; Young, D.; Ozin, G. A.; Bedard, R. L. *J. Mater. Chem.* **1998**, *8*, 711–720.

Published on Web 4/23/2009

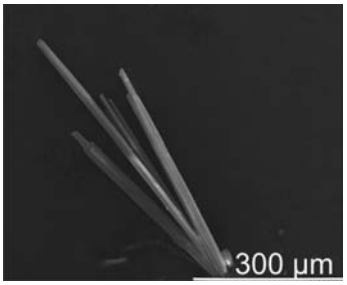

Figure 1. Scanning electron microscopy image of typical crystals of **1**.

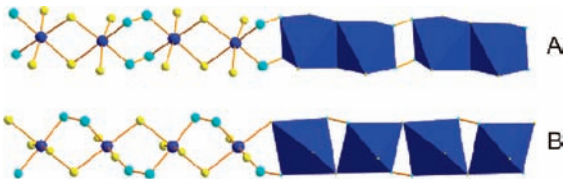

Figure 2. A (top) and B (bottom) chains in the structure of **1** viewed along the *a* axis. Color code: blue, Mn atoms; cyan, N atoms; yellow, S atoms.

with room temperature synthesis has been steadily increasing,[3,15] the use of hydrazine in the hydrothermal chemistry of metal chalcogenides has been little studied.[16] In general, studies employing hydrazine in hydrothermal conditions have mainly focused on the synthesis of nanocrystals.[17] Herein we give one of the first reports on the use of hydrazine in the solvothermal synthesis of new chalcogenide materials.

Compound **1** is formed in a hydrazine-rich aqueous environment as yellow needles (Figure 1) and crystallizes in the triclinic space group $P\bar{1}$.[18] In the structure of **1**, two different kinds of chains composed of linked MnL_6 (L = S, N) octahedra are easily recognized (Figure 2). These chains are stacked in the fashion ···ABAB··· along the *b* axis (Figure 3a). The A chain comprises $Mn_2S_6N_4$ dimers, which consist of MnS_4N_2 octahedra sharing a S···S edge. The dimers are interconnected via four ditopic hydrazine ligands to form the A chain along the *a* axis (Figure 2). Therefore, in **1**

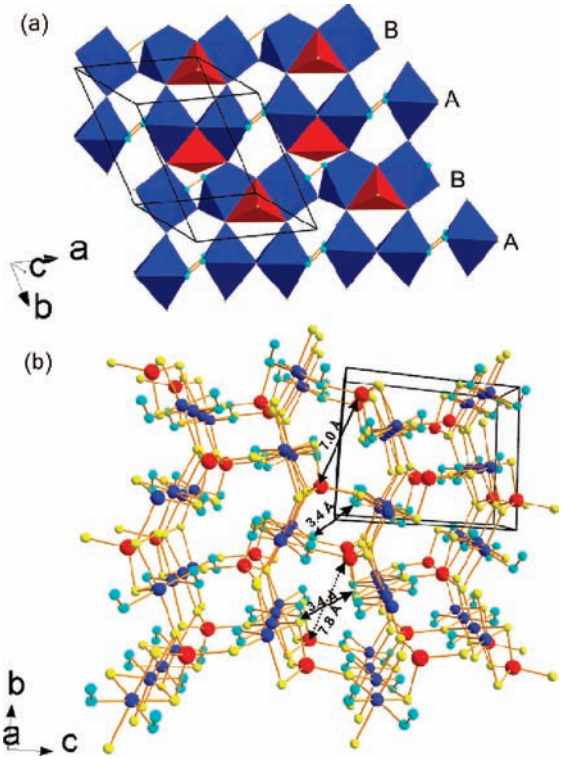

Figure 3. (a) Stacking and interconnectivity of A and B chains in the structure of **1** along the *a* and *b* axes. Color code: blue polyhedra, MnS_4N_2 octahedra; red polyhedra, SnS_4 tetrahedra; cyan balls, N atoms; yellow balls, S atoms. (b) View of the three-dimensional framework of **1** down the *a* axis with indication of the sizes of the pores (Mn, Sn, S, and N are represented by blue, red, yellow, and cyan balls, respectively). Mn−S and Mn−N bond distances lie in the ranges 2.531(3)−2.762(3) and 2.226(9)−2.310(9) Å, respectively. The Sn−S bond distances are found between 2.369(3) and 2.429(3) Å. The N−N bond distances are in the range 1.449(13)−1.465(13) Å.

the hydrazine molecules are an integral part of the framework and are not guest molecules inside the framework. The B chain consists of MnS_4N_2 octahedra sharing a corner (S) and further bridged through one H_2N-NH_2 ligand (Figure 2). The A and B chains are directly connected to each other along the *b* axis by the corner sharing of adjacent MnL_6 octahedra. SnS_4 tetrahedra share two corners with each of the $Mn_2S_6N_4$ dimers of the A chain and two edges with two adjacent MnS_4N_2 octahedra of the B chain. The remaining S atoms of the SnS_4 units bridge chains [adjacent A and B chains or neighboring chains of the same kind (A or B)] along the *c* axis, thus forming the three-dimensional framework (Figure 3b). The interconnectivity of the A and B chains creates two types of small pores and channels running along the *a* and *b* axes. One type is formed by two chains (two A or two B) and two SnS_4 tetrahedra and has dimensions 3.4 Å × 4.4−4.5 Å. The second type of pore with dimensions 3.4 Å × 7.0−7.8 Å is created by four chains (two A and two B) and four SnS_4 tetrahedra.

Interestingly, a hydrazine-free compound with the same stoichiometry (i.e., Mn_2SnS_4) is known,[19] and compound **1** can be regarded as a N_2H_4 insertion product in which the dense three-dimensional structure of Mn_2SnS_4 is expanded to a lower density architecture. It is also worth comparing the structure of compound **1** with that of the related material $[Mn_2SnS_4(N_2H_4)_5]$ (**2**).[15a] Although both compounds exhibit

(14) Synthesis of **1**: Elemental Sn (1 mmol, 0.120 g), Mn (2 mmol, 0.110 g), and S (4.5 mmol, 0.145 g), hydrazine monohydrate (2 mL, 98%), and distilled water (2 mL) were mixed in a 23 mL Teflon-lined stainless steel autoclave. ***Note!*** *Hydrazine is toxic and should be handled with care. Never mix metal nitrate salts with hydrazine because their mixture tends to explode violently upon heating*. The autoclave was sealed and placed in a temperature-controlled oven operated at 150 °C. The autoclave remained undisturbed at this temperature for 4 days. Then, the autoclave was allowed to cool at room temperature. A yellow crystalline product was isolated by filtration (0.28 g, yield ≈ 67% based on Sn), washed several times with water, acetone, and ether (in this order), and dried under vacuum. Energy-dispersive spectroscopy analysis on various needle-shaped crystals gave the average formula "$Mn_2SnS_{3.8}$". Elem anal. Calcd for $H_8N_4Mn_2SnS_4$: H, 1.92; N, 13.31. Found: H, 1.78; N, 12.57. The purity of the product was verified by powder X-ray diffraction (see the Supporting Information).

(15) (a) Yuan, M.; Dirmyer, M.; Badding, J.; Sen, A.; Dahlberg, M.; Schiffer, P. *Inorg. Chem.* **2007**, *46*, 7238–7240. (b) Mitzi, D. B. *Inorg. Chem.* **2005**, *44*, 7078–7086. (c) Mitzi, D. B. *Inorg. Chem.* **2005**, *44*, 3755–3761. (d) Mitzi, D. B. *Inorg. Chem.* **2007**, *46*, 926–931.

(16) Huang, X. Y.; Li, J.; Zhang, Y.; Mascarenhas, A. *J. Am. Chem. Soc.* **2003**, *125*, 7049–7055.

(17) Zhu, H. L.; Yang, D. R.; Yu, G. X.; Zhang, H.; Yao, K. H. *Nanotechnology* **2006**, *17*, 2386–2389.

(18) Crystals of **1** belong to the space group $P\bar{1}$ (No. 2) with a = 8.1603(19) Å, b = 10.253(3) Å, c = 12.693(3) Å, V = 966.8(4) Å^3, α = 84.54(2)°, β = 72.840(18)°, and γ = 72.328(18)°. Other crystal data: Z = 2, D_c = 2.836 mg/m^3, μ = 5.940 mm^{-1}; total reflections 14 452, independent reflections 4658, parameters 160 (R_{int} = 0.12); R1 = 0.0694, wR2 = 0.1445, GOF = 1.261.

(19) Partik, M.; Stingl, T.; Lutz, H. D. *Z. Anorg. Allg. Chem.* **1995**, *621*, 1600–1604.

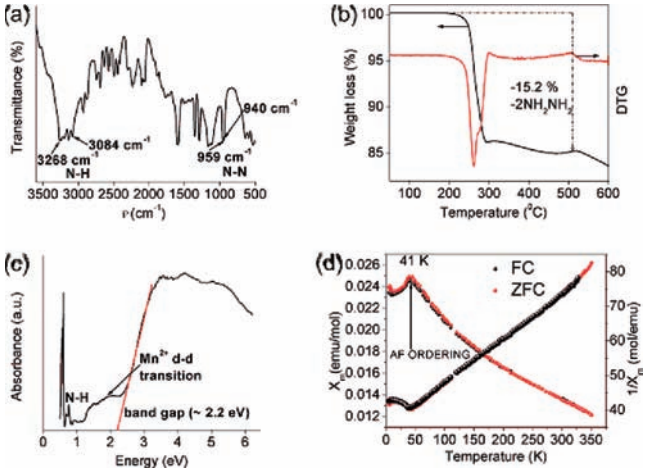

Figure 4. (a) Mid-IR spectrum of compound **1** with the presence of N−H and N−N stretches. (b) TGA and differential thermogravimetric curves for compound **1** (25−600 °C, N_2 atmosphere, heating rate 10 °C/min). (c) Solid-state near-IR/UV−vis spectrum of compound **1** with the assignment of various optical absorption features. A series of sharp peaks appear in the low-energy region (< 1 eV) and may be assigned to $\Delta v = 2$ overtones of hydrazine-related mid-IR stretches [e.g., the peak at ~6161 cm^{-1} (0.76 eV) is close to the $\Delta v = 2$ overtone of the N−H stretch at ~3083 cm^{-1}].[23] (d) Representation of zero-field-cooled (ZFC) and field-cooled (FC) magnetic susceptibility data for compound **1** (T = 5−330 K; H = 500 Oe). A linear fitting of the inverse ZFC susceptibility data from 53 to 329 K can be performed with the Curie−Weiss law [R^2 = 0.999; intercept = 34.36(8); slope = 0.1310 (4)], yielding $\mu_{eff} \sim 5.50\,\mu_B$ per Mn atom and Weiss temperature $\theta = -262$ K. Curie−Weiss fitting [R^2 = 0.999; intercept = 35.08(8); slope = 0.1280 (4)] of the inverse FC susceptibility data in the temperature range 49−327 K yielded $\mu_{eff} \sim 5.60\,\mu_B$ per Mn ion and Weiss temperature $\theta = -274$ K.

three-dimensional frameworks, their structural characteristics are substantially different. In compound **1**, as mentioned above, the interconnectivity of MnS_4N_2 octahedra includes corner (S) and edge (S···S) sharing and bridging through hydrazine ligands and SnS_4 tetrahedral units (sharing all of their S atoms). By comparison, the $MnSN_5$ octahedra in the less dense **2** are connected alternatively by two and three hydrazine bridges as well as SnS_4 units having two terminal (unshared) S ligands. For a side-by-side comparison of the structures of compounds **1** and **2**, see the Supporting Information.

Infrared (IR) spectroscopy indicates a number of peaks between 3083 and 3267 cm^{-1} assigned to N−H stretches (Figure 4a).[20] In addition, two peaks at 940 and 960 cm^{-1} are attributed to N−N stretches and are typical for compounds containing bridging H_2N-NH_2 ligands.[21] Thermogravimetric analysis (TGA) for compound **1** revealed no weight loss up to ~215 °C (Figure 4b). This is consistent with the absence of any free solvent molecules in the structure. A steep and significant (~13.8%) weight loss was observed between 215 and 300 °C, while a much smaller loss (~1.4%) happened between 300 and 510 °C. The total weight loss (~15.2%) in these two stages corresponds to the complete removal of the two hydrazine ligands of **1** (calculated weight loss = 15.2%). Pyrolysis mass spectroscopy revealed the release of hydrazine molecules at both ~250 and 480 °C and essentially confirmed our assignment of the thermal analysis data. The final product is presumably Mn_2SnS_4.[19]

Solid-state near-IR/UV−vis spectroscopy for compound **1** indicated a band-gap energy of ~2.2 eV (Figure 4c). In addition, a weak absorption feature is observed below the band-gap transition (at ~1.7 eV) and is attributed to midgap states associated with Mn^{2+} d−d transitions.[22]

The interconnectivity of magnetic d^5 Mn^{2+} centers via various diamagnetic bridges (μ_2-S^{2-} and μ_2-NH_2NH_2) as well as through SnS_4 units in **1** gives rise to a series of superexchange magnetic interactions. The magnetic data obey the Curie−Weiss law in the temperature range 50−330 K (Figure 4d). Linear fitting of the inverse susceptibility data yielded $\mu_{eff} \sim 5.5$−$5.6\,\mu_B$ per Mn ion, which is close to the calculated magnetic moment ($5.9\,\mu_B$) for Mn^{2+}. Remarkably, a very large negative Weiss temperature, $\theta \sim -262(5)$ K, was obtained, indicating strong antiferromagnetic (AF) interactions. A large negative Weiss temperature is also observed in Mn_2SnS_4 (θ = −463 K).[19] Below 50 K, the $1/\chi_m$ vs T curve significantly deviates from linearity. A clear peak is apparent in the susceptibility centered at ~41 K, indicating AF ordering of the Mn^{2+} ions consistent with significant "communication" between the magnetic centers.

Clearly, solvothermal conditions in hydrazine/water solutions offer the opportunity to stabilize novel materials such as **1**. It is also noteworthy that hydrazine is not protonated and acts as a neutral bridging ligand, in contrast to a counterion role of most amines used in the hydrothermal synthesis of chalcogenides. The strongly coordinating nature of hydrazine seems to suppress protonation and could allow for stabilization of new architectures.

Acknowledgment. Financial support from the National Science Foundation (Grant DMR-0801855) is gratefully acknowledged.

Supporting Information Available: Details for the physical and analytical techniques used in the present work, side-by-side comparison of the structures of compounds **1** and **2**, experimental versus calculated powder X-ray diffraction patterns of **1**, and a CIF file for **1**. This material is available free of charge via the Internet at http://pubs.acs.org.

(20) Crossland, J. L.; Zakharov, L. N.; Tyler, D. R. *Inorg. Chem.* **2007**, *46*, 10476–10478.
(21) Braibanti, A.; Dallavalle, F.; Pellinghelli, M. A.; Leporati, E. *Inorg. Chem.* **1968**, *7*, 1430–1433.
(22) Axtell, E. A.; Hanko, J.; Cowen, J. A.; Kanatzidis, M. G. *Chem. Mater.* **2001**, *13*, 2850–2863.
(23) Murray, M.; Kurtz, J. *J. Quant. Spectrosc. Radiat. Transfer* **1993**, *50*, 585–590.